

## Alpha-gamma decay studies of $^{255}\text{No}$

F.P. Heßberger<sup>1,a</sup>, S. Hofmann<sup>1,2</sup>, D. Ackermann<sup>1</sup>, S. Antalic<sup>3</sup>, B. Kindler<sup>1</sup>, I. Kojouharov<sup>1</sup>, P. Kuusiniemi<sup>1</sup>, M. Leino<sup>4</sup>, B. Lommel<sup>1</sup>, R. Mann<sup>1</sup>, K. Nishio<sup>5,1</sup>, A.G. Popeko<sup>6</sup>, B. Sulignano<sup>1,7</sup>, S. Saro<sup>3</sup>, B. Streicher<sup>3</sup>, M. Venhart<sup>3</sup>, and A.V. Yeremin<sup>6</sup>

<sup>1</sup> Gesellschaft für Schwerionenforschung (GSI), D-64220 Darmstadt, Germany

<sup>2</sup> Institut für Physik, Johann Wolfgang Goethe - Universität Frankfurt, D-60054 Frankfurt, Germany

<sup>3</sup> Department of Physics, Comenius University Bratislava, SK-84248 Bratislava, Slovakia

<sup>4</sup> Department of Physics, University of Jyväskylä, FIN-40014 Jyväskylä, Finland

<sup>5</sup> Japan Atomic Energy Agency (JAEA), Tokai, Ibaraki 319-1195, Japan

<sup>6</sup> Flerov Laboratory of Nuclear Reactions, JINR, RUS-141890 Dubna, Russia

<sup>7</sup> Institut für Physik, Johannes Gutenberg-Universität, D-55099 Mainz, Germany

Received: 2 May 2006 / Revised: 27 June 2006 /

Published online: 4 September 2006 – © Società Italiana di Fisica / Springer-Verlag 2006

Communicated by J. Äystö

**Abstract.** The decay of  $^{255}\text{No}$  was investigated by means of  $\alpha$ - $\gamma$  spectroscopy. The isotope was produced in the reactions  $^{208}\text{Pb}(^{48}\text{Ca}, n)^{255}\text{No}$ ,  $^{209}\text{Bi}(^{48}\text{Ca}, 2n)^{255}\text{Lr} \xrightarrow{EC} ^{255}\text{No}$ , and  $^{238}\text{U}(^{22}\text{Ne}, 5n)^{255}\text{No}$ . Levels of the daughter nucleus  $^{251}\text{Fm}$  were assigned by  $\alpha$ - $\gamma$  coincidence measurements and on the basis of systematics. Level energies were determined precisely using measured  $\gamma$ -rays. The results are compared with the known level schemes of the lighter  $N = 151$  isotones  $^{247}\text{Cm}$  and  $^{249}\text{Cf}$  as well as with data for  $^{253}\text{No}$ .

**PACS.** 23.60.+e Alpha decay – 27.90.+b  $220 \leq A < 250$  – 21.10.-k Properties of nuclei; nuclear energy levels

### 1 Introduction

In recent years the sensitivity of experiments for the study of nuclei produced in fusion reactions at low cross-sections was increased considerably. The improvements are based on higher beam intensities from accelerators, on higher efficiencies of electromagnetic devices for the separation of the reaction products in-flight, and on the improvement of detector systems for the simultaneous measurement of various decay modes of the produced nuclei. Detectors are mounted near the target for the study of promptly emitted radiation using the recoil decay tagging technique as well as in the almost background free focal plane of the separators. A review of recent results obtained in the region of elements  $Z \geq 100$  is given in [1]. Compared to the experiments which were performed two decades ago, the overall yield is now higher by one or two orders of magnitude. Therefore more detailed decay studies can be performed including highly efficient coincidence measurements between  $\alpha$  particles and  $\gamma$ -rays. Applying this method for the decay studies of the even- $Z$  isotopes  $^{255}\text{Rf}$  and  $^{253,251}\text{No}$  and their  $\alpha$ -decay products we extended the systematics of Nilsson levels in  $N = 145, 147, 149$  isotones for elements with proton numbers  $Z \geq 98$  [2, 3].

In the present work we obtained new results on the systematics of level schemes of the heavier series of odd- $N$  isotones,  $N = 151$ , by studying low-energy levels of  $^{251}\text{Fm}$ , populated by  $\alpha$  decay of  $^{255}\text{No}$ .

### 2 Experiment

The experiments using beams of  $^{48}\text{Ca}$  and  $^{22}\text{Ne}$  were performed at GSI, Darmstadt. The  $^{48}\text{Ca}$  beam was delivered by the high charge state injector with ECR ion source, while the  $^{22}\text{Ne}$  beam was delivered from the PIG ion source. Beam parameters and reactions used to produce the investigated nuclides are given in table 1. The targets were prepared from isotopically enriched material of  $^{208}\text{Pb}$  (enrichment 98.6%),  $^{238}\text{U}$  (> 99.5%), and  $^{209}\text{Bi}$ . Layers of (350–450)  $\mu\text{g}/\text{cm}^2$  thickness were evaporated on carbon foils of 40  $\mu\text{g}/\text{cm}^2$  (positioned upstream), which were then covered by evaporation of (5–20)  $\mu\text{g}/\text{cm}^2$  carbon. The target layer consisted of metallic lead or bismuth. In part of the irradiations  $\text{PbS}$  or  $\text{Bi}_2\text{O}_3$  compounds were used, because these materials withstood better highest beam currents due to their higher melting points [4]. The “uranium” targets were produced from  $\text{UF}_4$  compound. The targets were mounted on a wheel which rotated synchronously to the beam macro structure [5] (5 ms wide pulses at 50 Hz repetition frequency).

<sup>a</sup> e-mail: F.P.Hessberger@gsi.de

**Table 1.** Summary of beam parameters and reactions used for the production of  $^{255}\text{No}$  and  $^{253}\text{No}$ .

Projectile	Target (% enrichment)	Evaporation Residue	$E_{proj}/A$ MeV	$I/p\mu\text{A}^1$	$\epsilon_{SHIP}^2$	$\sigma/\text{nb}^3$
$^{22}\text{Ne}$	$^{238}\text{U}$ (> 99.5)	$^{255}\text{No}$	5.2	3.5	0.03	100
$^{48}\text{Ca}$	$^{208}\text{Pb}$ (98.6)	$^{255}\text{No}$	4.45	1.1	0.4	140
$^{48}\text{Ca}$	$^{209}\text{Bi}$	$^{255}\text{Lr}$ ( $\xrightarrow{EC} ^{255}\text{No}$ )	4.55	1.1	0.4	200

<sup>1</sup> Average beam intensity.<sup>2</sup> Calculated value of the separator efficiency.<sup>3</sup> Maximum value in the case of several bombarding energies.**Table 2.** Summary of decay data of  $^{255}\text{No}$ .

$E_\alpha/\text{keV}$	$i_{rel}$	HF	$E^*/\text{keV}^1$	$E_\gamma/\text{keV}$	$i_{rel}^2$	$T_{1/2}/\mu\text{s}^3$
$8290 \pm 20$	$0.05 \pm 0.02$	922	gs			
( $8255 \pm 20$ )	$0.03 \pm 0.02$	1110	( $35 + x$ )		(1)	
$8095 \pm 10$	$0.58 \pm 0.05$	16	200	$199.9 \pm 0.3$	1	$21 \pm 3$
$7941 \pm 10$	$\approx 0.004$	680	354	$353.8 \pm 0.4$	1	
$7903 \pm 10$	$0.11 \pm 0.03$	18	392	$192.1 \pm 0.3$	1	
$7893 \pm 20$	$0.04 \pm 0.02$	50	394	$194.5 \pm 0.5^4$	1	
$7742 \pm 10$	$0.19 \pm 0.04$	3	558	$358.3 \pm 0.3$	$0.18 \pm 0.04$	
				$166.8 \pm 0.4$	$0.51 \pm 0.13$	
				$163.3 \pm 0.4^5$	$0.31 \pm 0.8$	

<sup>1</sup> Excitation energy of the level populated by the  $\alpha$  decay; values are rounded.<sup>2</sup> Relative decay of the level including also conversion.<sup>3</sup> Only given for the isomeric state.<sup>4</sup> Level and decay energies are tentative.<sup>5</sup> Decay tentatively assigned to this level.

The evaporation residues leaving the targets with energies of  $\approx$  (40–50) MeV ( $^{48}\text{Ca}$ -induced reaction) or  $\approx$  (7–8) MeV ( $^{22}\text{Ne}$ -induced reaction) were separated from the primary beam by the velocity filter SHIP [6]. In the focal plane of SHIP they were implanted into a position-sensitive 16-strip PIPS detector (“stop detector”) with an active area of  $80 \times 35 \text{ mm}^2$  and a depletion depth of  $300 \mu\text{m}$  [7] for measuring the kinetic energies of the residues as well as subsequent  $\alpha$  decays [8,9]. Gamma rays emitted in prompt or delayed coincidence with  $\alpha$  decays were measured using a Clover detector consisting of four Ge crystals (70 mm  $\varnothing$ , 140 mm length), which were shaped and assembled to form a block of  $124 \times 124 \times 140 \text{ mm}^3$ .

Alpha calibration was performed using the decay energies of  $^{254}\text{No}$  and its daughter products  $^{250}\text{Fm}$  and  $^{246}\text{Cf}$ , produced in the reaction  $^{208}\text{Pb}(^{48}\text{Ca}, 2n)^{254}\text{No}$ , as described in detail in [10]. The accuracy of the calibration is estimated as  $\pm 20 \text{ keV}$ . Energy resolution of most of the strips was  $(23 \pm 3) \text{ keV}$  (FWHM), while for few ones it was only (40–55) keV (FWHM). Alpha data given in the text and in table 2 refer to strips with resolutions lower than 30 keV (FWHM) only.

In the case of populating excited levels that decay by internal conversion, one has to consider energy summing of  $\alpha$  particles and conversion electrons [3, 11]. It was found, however, that at full energy summing, the energy shift of

the  $\alpha$  lines is larger than the energy of the conversion electrons ( $E - E_B$ ) [11]. The reason is, that also part of the energy release of the atomic shell (Auger electrons, low-energy X-rays) contributes to the energy summing. This effect was investigated in more detail in the course of these studies and it was found that the energy shift can be approximately given as  $\Delta E \approx (E - E_B) + 0.5 \times (E_B - E_x)$ , when the conversion electron is fully stopped in the detector. Here  $E$  denotes the energy of the transition,  $E_B$  the electron binding energy (in case of  $L$ -,  $M$ -conversion the “averaged” value) and  $E_x$  the averaged X-ray energy. It should be emphasized that the formula has to be taken separately for  $K$ -,  $L$ - and  $M$ -conversion.

Gamma calibration was performed with standard energies from  $^{152}\text{Eu}$  and  $^{133}\text{Ba}$  sources. The accuracy of these calibration procedures was  $\pm 0.5 \text{ keV}$  for  $\gamma$  energies within one experimental run, while the values obtained in different experimental runs could be reproduced within  $\pm 1 \text{ keV}$ .

The intensities of the  $\gamma$  lines from the  $^{133}\text{Ba}$  decay were used to estimate the relative efficiency of the Ge detectors in the range of  $E_\gamma = (80\text{--}390) \text{ keV}$ , while the absolute  $\alpha$ - $\gamma$  coincidence efficiency ( $\epsilon_{\alpha\gamma}$ ) was estimated from the ratio of  $\alpha$ - $\gamma$  coincidences and  $\alpha$  singles measured for the coincident  $\alpha$ - and  $\gamma$ -rays of 8422 keV and 209.6 keV of  $^{247}\text{Md}$  and of 7540 keV and 293.7 keV of  $^{251}\text{Md}$  [12], respectively, as described in ref. [3].

The hindrance factor (HF) for an  $\alpha$  transition is defined as the ratio  $T_{\alpha,exp}/T_{\alpha,theo}$  with  $T_{\alpha,exp} = T_{1/2}/(b_{\alpha} \times i_{\alpha})$ , where  $T_{1/2}$  and  $b_{\alpha}$  denote the half-life and the  $\alpha$  branching of the parent state and  $i_{\alpha}$  is the intensity of the transition relative to all  $\alpha$  transitions. The theoretical half-life was calculated using the formula proposed by Poenaru *et al.* [13] with the parameter modification suggested by Rurarz [14]. Hindrance factors are usually divided into four categories characterizing equal and different structure of parent and daughter states (see, *e.g.*, [15] and references therein). Alpha transitions in odd mass nuclei, where the unpaired nucleon remains in the same orbital in the parent and daughter nucleus, are characterized by low hindrance factors of 1–4 (favoured transitions).

Gamma decays were measured in prompt or delayed coincidence with  $\alpha$  decays. The limit for prompt coincidences of ( $\Delta t(\alpha-\gamma) < 1 \mu\text{s}$ ) was given by the time resolution of the detector set-up. Delayed coincidences were divided into two groups, the first for the time interval  $1 \mu\text{s} < \Delta t(\alpha-\gamma) < 4 \mu\text{s}$ , the second for the time interval  $\Delta t(\alpha-\gamma) > 16 \mu\text{s}$ . The first interval was defined by the internal coincidence time of the data acquisition system, the second one by the minimum time to register consecutive events due to the dead time of the data acquisition system. According to Weisskopf estimations of lifetimes [16], prompt coincidences between  $\alpha$  and  $\gamma$  decays are only expected for  $E1$ ,  $E2$ , and  $M1$  transitions.

Multipolarities of electromagnetic transitions were estimated on the basis of conversion coefficients.  $K$ -conversion coefficients can be derived from the ratio of  $\gamma$ - and X-ray events from a specific transition, since  $K$ -fluorescence yields  $\omega_K$  are close to unity for the heaviest nuclei. Determination of  $L(+M)$ -conversion coefficients is more complicated. We use the shift of  $\alpha$  lines due to energy summing between  $\alpha$  particles and conversion electrons. Principally  $L(+M)$ -conversion coefficients can be obtained from the intensity ratio of “shifted” and “unshifted” lines (see, ref. [3] for details). Although this method does not allow to determine the conversion coefficients precisely, in conjunction with the determination of  $K$ -conversion coefficients, the accuracy is sufficient to distinguish  $E1$ ,  $E2$  and  $M1$  transitions. Theoretical conversion coefficients were taken from [17]. Vice versa, using the known multipolarity of a transition, one is able to model the influence of energy summing with the  $\alpha$  lines, *i.e.* to model energy shifts and intensity ratios of unshifted and shifted lines, also with respect to different energies of electrons according to  $K$ -,  $L$ - and  $M$ -conversion.

### 3 Experimental results and discussion

#### 3.1 Decay of $^{255}\text{No}$

A partial level scheme of  $^{251}\text{Fm}$  was reported by Eskola *et al.* [18] on the basis of an  $\alpha$ -decay study of  $^{255}\text{No}$ . Spin and parity assignments were suggested in analogy with the decay of  $^{253}\text{Fm}$  [19]. This decay scheme served as a basis for our measurements. It is shown in fig. 1 with energies determined from our experiment and with our tentative

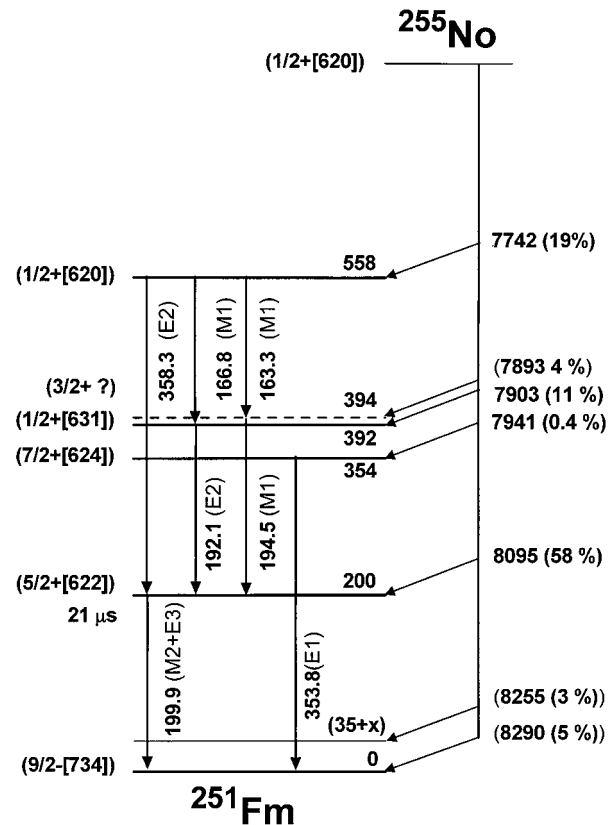


**Fig. 1.** Partial level scheme of  $^{251}\text{Fm}$  as derived from [18] and from this work. All energies are given in keV.

assignments for spin, parity, and Nilsson quantum numbers for the level at 392 keV and the new levels at 354 keV and 394 keV identified in this work. The dominant  $\alpha$  transition (58%) with an energy of 8.095 MeV was assigned to populate an excited state at 200 keV, whereas a weak transition (5%) of 8.29 MeV populates the ground state. In order to unambiguously identify the element assignment of the measured  $\alpha$  decays, Dittner *et al.* [20] performed  $\alpha$ -X-ray coincidence measurements which revealed a 191 keV level to be an isomeric state with a half-life of  $15.2 \mu\text{s}$ . The authors also observed a  $(187.2 \pm 0.2)$  keV  $\gamma$  line (192.1 keV in fig. 1) in prompt coincidence with  $\alpha$  particles of 7.927 and 7.879 MeV (7.903 MeV in fig. 1), which was assigned to populate the isomeric state [21]. The decay of the isomeric state was suggested to be of the multipolarity  $M2$  based on the earlier assigned spin and parity of isomer and ground state. The transition energy of 191 keV (200 keV in fig. 1) was derived from the energy difference of  $\alpha$  particles populating these levels and thus had a relatively large error bar. Overlapping  $\alpha$  lines between 7.620 and 8.312 MeV (not shown in fig. 1) were disentangled numerically, which resulted in a total of ten  $\alpha$  transitions with intensities between 1.9 and 45.5%.

On the basis of their results Bemis *et al.* [21] presented a more detailed partial level scheme than [18] also including excited members of rotational bands. Since transitions from excited members into the band heads are highly con-

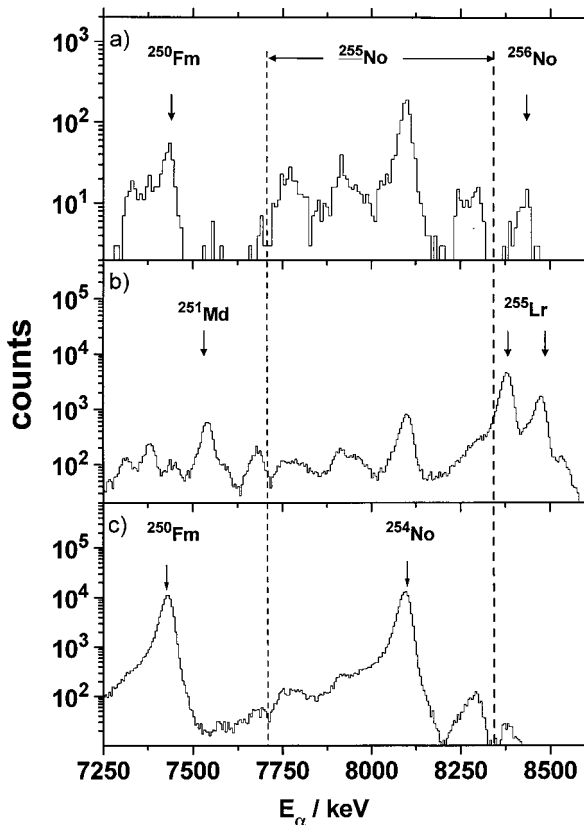


**Fig. 2.** Alpha spectra measured in the reactions  $^{238}\text{U}(^{22}\text{Ne}, 5n)^{255}\text{No}$  (a),  $^{209}\text{Bi}(^{48}\text{Ca}, 2n)^{255}\text{Lr}$  (b), and  $^{208}\text{Pb}(^{48}\text{Ca}, 1n)^{255}\text{No}$  (c).

verted and thus due to energy summing in our experiments those  $\alpha$  particles cannot be discriminated from  $\alpha$  decays into the band head, we could not reproduce the “fine structure” data given in [21]. The implantation method thus leads to a loss of information regarding energies of levels within a rotational band, populated by the  $\alpha$  decay. Those structures can be seen clearly, *e.g.* in the decay pattern of the  $N = 153$  isotope  $^{251}\text{Cf}$  [22].

In our study we remeasured the  $\alpha$ -decay scheme of  $^{255}\text{No}$  including  $\gamma$  detectors of high efficiency in order to establish a more accurate low-energy level scheme of  $^{255}\text{Fm}$ . The parent nucleus  $^{255}\text{No}$  was produced by the reactions  $^{238}\text{U}(^{22}\text{Ne}, 5n)^{255}\text{No}$ ,  $^{208}\text{Pb}(^{48}\text{Ca}, n)^{255}\text{No}$  and  $^{209}\text{Bi}(^{48}\text{Ca}, 2n)^{255}\text{Lr}$  and subsequent electron capture (EC) decay of  $^{255}\text{Lr}$ . For the  $^{255}\text{Lr}$  EC branch we obtained a value of 37% from the  $\alpha$  intensities of the  $^{255}\text{Lr}$  ground-state decay and the  $\alpha$  decay of its EC daughter  $^{255}\text{No}$  which itself has a known  $\alpha$  branching of 61.4% [16].

Problems in analyzing the  $\alpha$  spectra arose from the presence of decays of  $^{254}\text{No}$  having an  $\alpha$  energy (8.088 MeV) similar to the most intense line of  $^{255}\text{No}$  (8.095 MeV). The cleanest  $\alpha$  spectra were obtained from the production by  $^{238}\text{U}(^{22}\text{Ne}, 5n)^{255}\text{No}$  (fig. 2a), but also here we observed an  $\approx 30\%$  contribution of  $^{254}\text{No}$ , as seen from the intensity of its daughter product  $^{250}\text{Fm}$ . For the production by EC decay of  $^{255}\text{Lr}$  the transitions at (8.2–

8.3) MeV are overlaid by low-energy tails (or lines) of the  $\alpha$  spectrum of  $^{255}\text{Lr}$  (fig. 2b). Finally, in the reaction  $^{208}\text{Pb}(^{48}\text{Ca}, n)^{255}\text{No}$  only the  $\alpha$  transitions at (8.2–8.3) MeV and  $< 7.8$  MeV are visible, the others are covered by  $\alpha$  decays of the 2n channel ( $^{254}\text{No}$ ) which had an about a factor of three higher cross-section than the 1n channel (fig. 2c). But also in this reaction clean  $\alpha$ - $\gamma$  spectra were obtained for prompt coincidences. In the case of delayed coincidences the production via EC decay of  $^{255}\text{Lr}$  was more suitable for investigating the decay of the isomeric state in  $^{251}\text{Fm}$  than the direct production via  $^{208}\text{Pb}(^{48}\text{Ca}, n)^{255}\text{No}$ , although the production cross-section roughly was a factor of 2.5 lower, since it turned out that in the latter production the spectra were severely contaminated by random coincidences of 8.088 MeV  $\alpha$  decays of  $^{254}\text{No}$  and background  $\gamma$ -rays.

Evidently, the  $\alpha$  lines below 8.0 MeV are broad indicating a strong influence of energy summing with conversion electrons. This effect renders estimation of line intensities and thus the determination of  $\alpha$ -decay hindrance factors more difficult. Nevertheless, we estimated values by correcting distortions due to energy summing with conversion electrons on the basis of model calculations after having established the multiplicities of the internal transitions. The results are listed in table 2. Within the error bars they are in agreement with the results of [18, 21].

Gamma spectra observed in delayed ( $\Delta t(\alpha\text{-}\gamma) = (16\text{--}100) \mu\text{s}$ ) and prompt coincidence with  $\alpha$  decays of  $^{255}\text{No}$  (bordered by the dashed lines in fig. 2) are shown in figs. 3a and b, respectively. For aid of the following discussion a two-dimensional plot of prompt  $\alpha$ - $\gamma$  coincidences is shown in fig. 4.

The 199.9 keV  $\gamma$  line measured in delayed coincidence with  $\alpha$  particles (fig. 3a) is energetically clearly separated from the 192.1 keV line which is in prompt coincidence (fig. 3b). From the time differences between  $\alpha$  and delayed 199.9 keV  $\gamma$  decays or  $K$ -X-rays from fermium, we obtain a half-life of  $(21 \pm 3) \mu\text{s}$  for the emitting state. This value is still compatible with the literature value of  $(15.2 \pm 2.3) \mu\text{s}$  measured by Dittner *et al.* [20]. The energy of the delayed coincident  $\gamma$  line reveals that the energy of the isomeric state is at 200 keV and thus somewhat larger than the value of 191 keV given in ref. [20]. From our intensity ratios between  $K$ -X-rays and the 199.9 keV  $\gamma$  line we determine a conversion coefficient of  $\alpha_K = 8.3 \pm 2.9$ . This value is not in agreement with a pure  $M2$  transition, but requires an  $M2 + E3$  mixing and a mixing ratio of  $\approx 0.5$  using  $M2$ -,  $E3$ -conversion coefficients from [17] and the relation  $\alpha_K = a \times \alpha_K(M2) + (1 - a) \times \alpha_K(E3)$ .

Besides the  $K$ -X-rays from fermium two strong  $\gamma$  lines at  $E_\gamma = 192.1$  and 358.3 keV and three weaker lines at  $E_\gamma = 163.3$ , 166.8 and 353.8 keV are observed in prompt coincidence with  $\alpha$  transitions of  $E_\alpha = (7.7\text{--}8.0)$  MeV as seen in figs. 3b and 4a-d, which originate from levels above the isomer. The total decay energies of the transitions including the 358.3 keV and the 353.8 keV  $\gamma$ -rays are  $E = (Q_\alpha + E_\gamma) = 8.225$  MeV and  $E = 8.423$  MeV. These values are close to the  $Q$  value  $Q_\alpha(\text{iso}) = 8.224$  MeV for the  $\alpha$  decay into the isomeric state and the sum

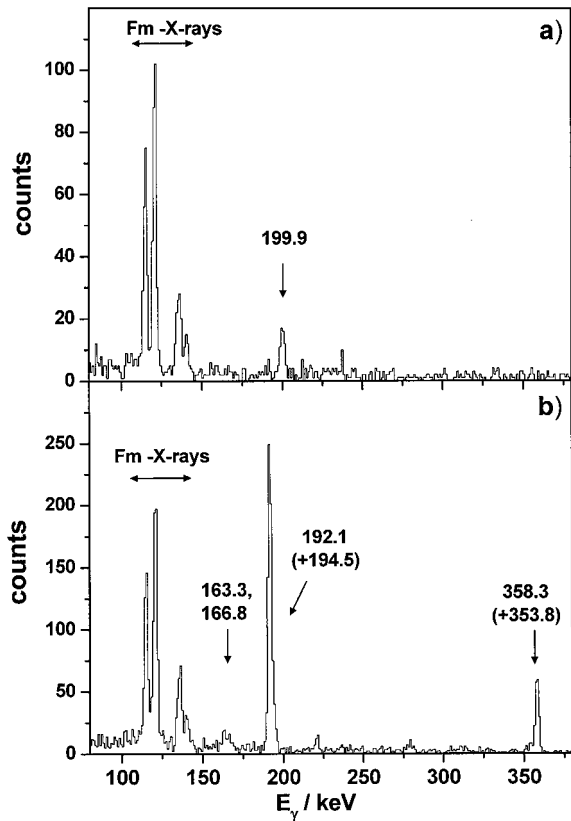


**Fig. 3.** Gamma spectra observed in delayed (a) and prompt (b) coincidence with  $\alpha$  decays of  $^{255}\text{No}$ .

$Q_{\alpha}(\text{iso}) + E_{\gamma}(\text{iso}) = 8.424 \text{ MeV}$ . Thus we regard the line at 358.3 keV as a transition into the isomeric state and the transition at 353.8 keV as a transition into the ground state. According to the suggested spins and parities for the levels at 558 keV and the isomeric state at 200 keV (see fig. 1) we assign the multipolarity  $E2$  to the 358.3 keV transition. Assignment of the 353.8 keV line is based also on the assumption that this line could only be observed because the transition into the ground state is favoured over the transition into the isomeric state. The spin and parity assignments for the latter states thus exclude spins of  $5/2^+$  or lower for the emitting state. Respecting that its lifetime must be lower than  $1 \mu\text{s}$  due to the  $\gamma$  decays observed in prompt coincidence with  $\alpha$  particles possible multiplicities of the transition are  $E1$ ,  $E2$  and  $M1$ . For an  $M1$  transition one expects a conversion coefficient  $\alpha_K \approx 1.3$  at 353.8 keV. Full energy summing between  $\alpha$  particles and conversion electrons of such a transition leads to an “effective”  $\alpha$  energy of  $\approx 8165 \text{ keV}$ . However, no coincidences of  $\alpha$  decays of that energy with  $K$ -X-rays were observed. Thus,  $M1$  multipolarity can be excluded. Possible remaining spin and parities are  $7/2^+$ ,  $9/2^+$ ,  $11/2^+$  ( $E1$  transitions), and  $13/2^-$  ( $E2$  transition). We tentatively assign  $7/2^+[624]$  to the emitting state since this Nilsson level has been observed in the lighter isotones at similar excitation energies. It is also expected below 500 keV from theoretical calculations (see sect. 3.2).

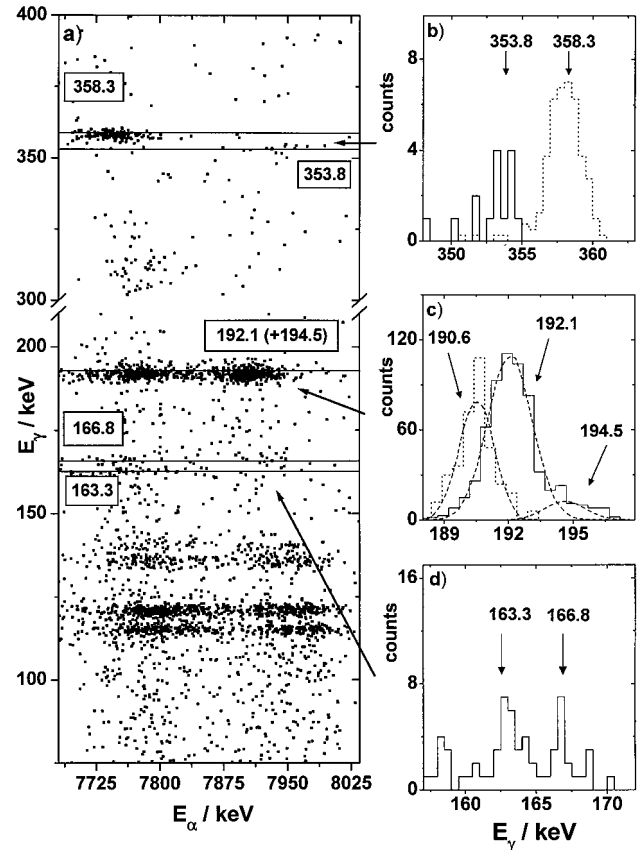


**Fig. 4.** a) Alpha-gamma correlation plot for prompt coincidences assigned to the decay of  $^{255}\text{No}$ , b)–d) projections on the  $\gamma$  energy axis; b) gamma spectrum in the energy range (348–363) keV; dotted line: energy of  $\gamma$ -rays coincident with the 7742 keV  $\alpha$  transition, full line: energy of  $\gamma$ -rays coincident with the 7941 keV  $\alpha$  transition; c) full line: gamma energy spectrum in the range (188–197) keV, dotted line: energy distribution of the 190.6 keV  $\gamma$ -rays in coincidence with  $\alpha$  decays of  $^{256}\text{Lr}$ , the dashed lines are results of Gaussian fits. d) Gamma energy spectrum in the range (157–172) keV.

A line at  $(187.2 \pm 0.2) \text{ keV}$  reported in [20,21] is obviously identical with the line for which we derived a new energy value of  $(192.1 \pm 0.3) \text{ keV}$  in this experiment. Arguments for assignments of this line and the weaker ones of 163.3 keV and 166.8 keV are the following: On the basis of energy balance we place the  $\gamma$  transitions of 192.1 keV and 358.8 keV into the level scheme as shown in fig. 1. Due to the agreement  $E_{\gamma}(\text{sum}) = (166.8 + 192.1) \text{ keV} = (358.9 \pm 0.5) \text{ keV}$  with the value of the  $(358.3 \pm 0.3) \text{ keV}$  line the  $\gamma$  line of 166.8 keV is interpreted as a transition between the  $E^* = 558 \text{ keV}$  and  $E^* = 392 \text{ keV}$  levels. An intense transition between these levels is indicated by a high coincidence rate (about 45% of the total) between the 192.1 keV line with  $\alpha$  particles below 7.88 MeV. The weak intensity of the 166.8 keV  $\gamma$  line indicates that this transition is highly converted. This assumption is corroborated by  $\alpha$ - $\gamma$ - $\gamma$  coincidence measurements. We obtain a lower limit of the intensity ratio (which can be interpreted as a lower limit for the  $K$ -conversion coefficient of the

166.8 keV transition) for prompt coincidences  $i(K\text{-X-ray} - \gamma(192.1\text{ keV}))/i(\gamma(166.8\text{ keV}) - \gamma(192.1\text{ keV})) > 7$  indicating a magnetic transition. With respect to the observation in prompt coincidence with  $\alpha$  particles and the discussion above we tentatively assign the multipolarity  $M1$  to it. The existence of a transition between the  $E^* = 558\text{ keV}$  and  $E^* = 392\text{ keV}$  levels is also in agreement with the energy shift (due to energy summing with conversion electrons) of the  $\alpha$  particles in  $\alpha\text{-}\gamma\text{-}\gamma$  coincidence (with  $K\text{-X-rays}$  and  $192.1\text{ keV}$   $\gamma$  transitions) compared to the energy (7.742 MeV) of the  $\alpha$  decays into the 558 keV level. We obtain a value of  $\Delta E \approx 35\text{ keV}$ , which, on the basis of the discussion in sect. 2, is expected for a transition energy of  $\approx 165\text{ keV}$ .

An upper limit for the total conversion coefficient of the 192.1 keV transition can be obtained from the ratio of  $\alpha$  particles and  $\alpha\text{-}\gamma(192.1\text{ keV})$  coincidences in the range below the  $\alpha$  energy for the “direct” population of the 392 keV level ( $E_\alpha < 7.88\text{ MeV}$ ) (see fig. 4a for illustration). Gamma decay events of 192.1 keV coincident with  $\alpha$  particles in this energy range are connected to a population of the 392 keV level by decay of the 558 keV level. So, the intensity ratio  $(\Sigma\alpha - \Sigma\alpha(358) + \Delta\alpha)/(\Sigma\gamma/\epsilon + \Delta(\alpha\text{-}\gamma))$  represents the total conversion coefficient of the 192.1 keV transition, provided the 558 keV level decays only by the 358.3 keV and 166.8 keV transitions. Since the latter cannot be assumed *a priori*, the obtained value represents an upper limit. In the relation above,  $\Sigma\alpha$  is the total number of  $\alpha$  decays in the considered interval,  $\Sigma\alpha(358)$  the number of  $\alpha$  decays attributed to the 358.3 keV transition.  $\Delta\alpha$ ,  $\Delta(\alpha\text{-}\gamma)$  represent the numbers of  $\alpha$  events and  $\alpha$  events in coincidence with 192.1 keV  $\gamma$ -rays shifted into the region  $E_\alpha > 7.88\text{ MeV}$  by energy summing with conversion electrons.  $\Sigma\gamma$  represents the number of  $\gamma$  events at 192.1 keV and  $\epsilon$  the efficiency of the Clover detector. However, the correction terms  $\Delta\alpha$  and  $\Delta(\alpha\text{-}\gamma)$  are dependent on the multiplicities of the 192.1 keV and 166.8 keV transitions. Using  $M1$  for the latter as assumed above, we obtain upper limits for the total conversion coefficients of  $\alpha(E1) < 2.2$ ,  $\alpha(M1) < 2.9$ ,  $\alpha(E2) < 3.7$  for the 192.1 keV transition. Theoretical conversion coefficients [17] are 0.1 ( $E1$ ), 1.7 ( $E2$ ) and 7.5 ( $M1$ ). Therefore  $M1$  can be excluded. The distinction between  $E1$  and  $E2$  can be obtained from the energy distribution of the  $\alpha$  particles in coincidence with the  $\gamma$  decays of 166.8 keV. Energy summing with  $L$ ,  $M$ -conversion electrons will shift the energy of the  $\alpha$  particles into the interval  $E_\alpha > 7.88\text{ MeV}$ . According to the  $L$ - and  $M$ -conversion coefficients from [17], we expect a ratio  $\Sigma(\alpha\text{-}\gamma)(E_\alpha < 7.88\text{ MeV})/\Sigma(\alpha\text{-}\gamma)(E_\alpha > 7.88\text{ MeV}) = 0.5$  for  $E2$  and  $< 0.05$  for  $E1$ . So, the experimental result of  $\approx 0.5$  suggests an  $E2$  transition.

Keeping spin and parity assignments of Eskola *et al.* [18] possible values for the level populated by an  $M1$  transition (166.8 keV) are  $1/2^+$  or  $3/2^+$ . Keeping the assignment  $5/2^+[622]$  for the isomeric level and respecting  $E2$  multipolarity for the 192.1 keV transition, a spin and parity assignment  $1/2^+$  is preferred. According to experimental assignments in  $^{247}\text{Cm}$  and  $^{249}\text{Cf}$  and the theoretical calculations presented in sect. 3.3 the Nilsson levels

$1/2^+[631]$  and  $1/2^+[620]$  are expected at low excitation energies in  $N = 151$  isotones. Since the level at 558 keV has already been attributed to  $1/2^+[620]$ , we tentatively assign  $1/2^+[631]$  to the 392 keV level, contrary to Bemis *et al.* [21] who assigned  $7/2^+[613]$ .

However, the assignments above cannot explain the ratio of  $\gamma(192.1\text{ keV})$  and  $K\text{-X-ray}$  events coincident with  $\alpha$  decays in the range  $E_\alpha < 7.88\text{ MeV}$  and the ratio of  $K\text{-X-ray}$  events coincident with  $\alpha$  decays in the range  $E_\alpha < 7.88\text{ MeV}$  to those  $E_\alpha > 7.88\text{ MeV}$ ; see fig. 4 for illustration. On the basis of model calculations we expect ratios  $i(K\text{-X})/i(\gamma)(E_\alpha < 7.88) = 1.5$  and  $i(K\text{-X}, (E_\alpha < 7.88))/i(K\text{-X}, (E_\alpha > 7.88)) = 2.15$ . Experimentally, we obtain values of 1.99 and 1.21. This indicates both an excess of X-rays compared to  $\gamma$  decays in the range  $E_\alpha < 7.88$  as well as an excess of X-rays in the range  $E_\alpha > 7.88\text{ MeV}$  compared to  $E_\alpha < 7.88\text{ MeV}$ . This suggests either a “third decay path” of the level at 558 keV or a level close to it populated significantly by  $\alpha$  emission. This assumption is corroborated by  $\alpha\text{-}\gamma\text{-}\gamma$  coincidence measurements. Taking coincidences  $K\text{-X-rays} - K\text{-X-rays}$  and  $K\text{-X-rays} - 192.1\text{ keV}$   $\gamma$  decays we obtain an intensity ratio  $i(K\text{-X} - K\text{-X})/i(K\text{-X} - \gamma(192.1)) = 1.3$ , while in case of only one decay sequence (166.8 keV - 192.1 keV) the ratio should reflect the  $K$ -conversion coefficient for the 192.1 keV transition, *i.e.*  $\approx 0.14$  for  $E2$ . This suggests that the additional transition is highly  $K$  converted. Tentatively, we attribute it to the weak 163.3 keV line (see fig. 4d). The energy distribution of the  $\alpha$  particles coincident to that line is similar to that of the 166.8 keV line in the range  $E_\alpha < 7.88\text{ MeV}$ , except that the component above this energy is almost missing, as indicated in fig. 4a.

On the basis of the present data only a tentative assignment can be given. The observation of strong coincidences between  $K\text{-X-rays}$  and the lack of intense  $\gamma$  lines suggest a two-step decay, populating an isomeric state, since no prompt  $\gamma$ 's that could indicate a decay into the ground state have been observed. The energy of this isomeric state can be only slightly different ( $\approx 20\text{--}30\text{ keV}$ ) to 200 keV since we did not observe significant differences in the energy distribution of  $\alpha$  particles in delayed coincidence with X-rays and the 199.9 keV transition. On the other hand, we do not observe a clear  $\gamma$  line that could represent the decay into such an isomeric level. However, a hint for such a transition could be the pronounced shoulder at the high-energy side of the 192.1 keV line which is not present for the 190.6 keV line coincident with  $\alpha$  decays of  $^{256}\text{Lr}$ , measured in the same experiment, and thus the shoulder cannot be explained as due to detector deterioration (see fig. 4c). A two-Gaussian fit to the energy distribution delivers a value 194.5 keV for the “shoulder line”, indicating a “sum energy” for both transitions of 357.6 keV, a value close to the energy difference of the 558.3 keV and 199.9 keV levels. The conversion probability of the transitions of this decay path suggests that both are  $M1$ . One possible explanation is to assume an  $\alpha$  transition branch into the  $3/2^+$  member of the rotational band built up on the  $1/2^+[620]$  Nilsson level followed by decay via the  $3/2^+$  member of the rotational band built up

on the  $1/2^+[631]$  level into the isomeric state. This interpretation, however, is somewhat in conflict with the energy systematics of the  $3/2^+$  members of the bands built up on the  $1/2^+[631]$  and  $1/2^+[620]$  levels. Typical energy differences are  $\Delta E(3/2^+-1/2^+) \approx 10$  keV for  $1/2^+[631]$  and  $\Delta E(3/2^+-1/2^+) \approx 25$  keV for  $1/2^+[620]$ , so one would rather expect transition energies of  $\approx 180$  keV and  $\approx 200$  keV instead of 163.3 keV and 194.5 keV. Although this is not fully proven so far on the basis of the present data, we do not suggest another isomeric level close to 200 keV but rather a “third decay path” of the  $1/2^+[620]$  level into the  $5/2^+[622]$  isomeric state, running via a so far unknown level at 394 keV, as shown in fig. 1.

The  $\alpha$  decays above 8.2 MeV were not in coincidence with  $\gamma$ -rays or X-rays. They are interpreted as decays into levels below the isomer. In refs. [18,20,21] two  $\alpha$  lines were observed and interpreted as decays into the  $9/2^-$  ground state of  $^{251}\text{Fm}$  and the  $11/2^-$  member of the rotational band built up on it, which was placed at  $E^* \approx 50$  keV [18] or  $E^* = 46$  keV [20,21]. The intensity of the  $\alpha$  decay into the  $11/2^-$  state was roughly a factor of two higher than that of the decay into the ground state. We observed a broad line, which numerically was disentangled into two components of 8290 keV and 8255 keV. The intensities were reversed compared to the previous results [18,20,21]. We interpret this seeming discrepancy by energy summing between conversion electrons from the  $M1$  transition  $11/2^- \rightarrow 9/2^-$  and  $\alpha$  particles, which apparently increases the intensity of the transition into the ground state. It also feigns a lower energy of the  $11/2^-$  level, due to a higher  $\alpha$  energy caused by energy summing with the energy loss signal of conversion electrons escaping the detector. We thus denote it as  $(35 + x)$  keV and give the value in brackets in fig. 1 and in table 2.

### 3.2 Systematics of nuclear levels in $N = 151$ isotones

Low-lying Nilsson levels in odd mass nuclei with even atomic numbers are essentially determined by the unpaired neutron. Thus,  $\alpha$  decay patterns and low-lying excited levels exhibit similarities in isotonic nuclei. Figure 5a shows the situation for the  $N = 151$  isotones  $^{247}\text{Cm}$ ,  $^{249}\text{Cf}$ ,  $^{251}\text{Fm}$ , and  $^{253}\text{No}$  on the basis of experimental assignments. Data for  $^{251}\text{Fm}$  are from this study, while those for  $^{247}\text{Cm}$  and  $^{249}\text{Cf}$  are taken from [22,16]. Data for  $^{253}\text{No}$  are less certain so far. First, information on levels in this isotope were obtained from  $\alpha$ -decay studies of  $^{257}\text{Rf}$  [23,24]. Its decay scheme, however, was later revised on the basis experiments performed at SHIP, which identified the two  $^{257}\text{Rf}$   $\alpha$  lines of highest energy as due to decay of an isomeric state, while the  $5/2^+[622]$  was settled at  $E^* \approx 120$  keV on the basis of energies of  $\alpha$  decays attributed to ground-state-to-ground-state transitions [25]. More detailed studies of the decay of  $^{257}\text{Rf}$ , including  $\alpha$ - $\gamma$  coincidence measurements, performed at SHIP recently, however, indicate that the  $5/2^+[622]$  level has to be settled at an about 50 keV higher energy [26]. An in-beam study of  $^{253}\text{No}$  was performed by Reiter *et al.* [27]. They observed a series of  $\gamma$  transitions that were interpreted as

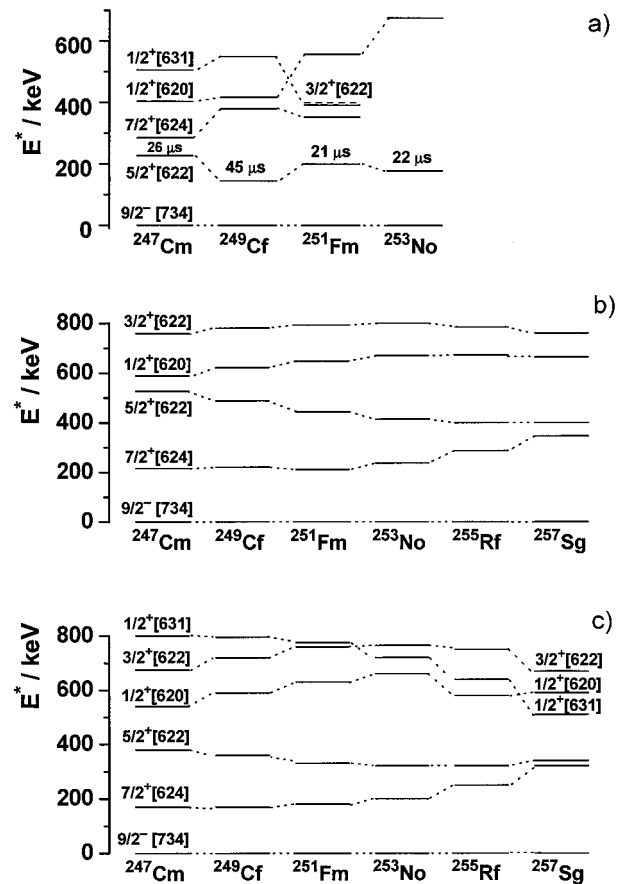


**Fig. 5.** Systematics of low-lying levels of  $N = 151$  isotones; a) experimental assignments based on [18] and this work, b) results of calculations by Cwiok *et al.* [28], c) results of calculations by Parkhomenko and Sobiczewski [29].

due to the rotational band built up on the  $7/2^+[624]$  Nilsson level. The energy of the band head was tentatively settled at  $E^* \approx 355$  keV. However, this value was not supported in a recent study of  $^{253}\text{No}$  performed by our group. Therefore, the level is omitted in fig. 5a.

Figures 5b, c display the results of theoretical predictions by Cwiok *et al.* [28] and Parkhomenko *et al.* [29]. From experimental side only the  $9/2^- [734]$  ground state and the  $5/2^+[622]$  state are well established for all four nuclei. The isomeric character, the similar excitation energies and the similar half-lives strongly suggest the same configurations for the initial and final states. In the calculations the positions of the  $5/2^+[622]$  and the  $7/2^+[624]$  are interchanged. Therefore isomeric states do not appear. Experimentally, the  $7/2^+[624]$  level had been identified in  $^{247}\text{Cm}$  and  $^{249}\text{Cf}$  and was found to decay predominantly via  $E1$  transitions into the ground state. In our experiment the assignment in  $^{251}\text{Fm}$  was based on the properties of the populating  $\alpha$  transition and the depopulating  $\gamma$  transition. Although in both cases the assignment has to be regarded as tentative it seems the appropriate choice, exhibiting an increase in energy from  $^{247}\text{Cm}$  to  $^{249}\text{Cf}$  followed by smooth decrease with increasing atomic number.

This behavior is approximately reproduced by the calculations, which predict a steady increase with increasing atomic number.

The most striking feature in fig. 5a is the steep increase of the energy of the  $1/2^+[620]$  states from  $^{249}\text{Cf}$  to  $^{253}\text{No}$ . The latter state originates from the  $2g_{7/2}$  neutron orbital and the Nilsson diagram exhibits a steep decrease of its energy with increasing deformation ( $\epsilon_2$ ) (see, *e.g.*, [16]), which means, the behavior shown in fig. 5a may indicate a steady decrease in deformation from  $^{249}\text{Cf}$  to  $^{253}\text{No}$ . This, however, is not in line with the calculations which rather indicate similar deformations for the  $N = 151$  isotones from  $^{247}\text{Cm}$  to  $^{253}\text{No}$  of  $\beta_2 = 0.235\text{--}0.245$  [30],  $\beta_2 = 0.244\text{--}0.250$  [28] or  $\beta_2 = 0.242\text{--}0.252$  [29]. Also the level energies are predicted to change only slightly as seen in figs. 5b,c. Since in sect. 3.1, finally, only spin and parity of the levels at 558 keV and 392 keV were assigned, it seems tempting to exchange the asymptotic quantum numbers for both levels, *i.e.* to denote the level at 391 keV as  $1/2^+[620]$  and that at 558 keV as  $1/2^+[631]$ , which would result in a smoother trend in the energies of both levels from  $^{247}\text{Cm}$  to  $^{251}\text{Fm}$ , as also predicted by the calculations for  $1/2^+[620]$ . While there are no predictions for  $1/2^+[631]$  in [28] over a wide range of  $N = 151$  isotones, [29] predict a smooth decrease of this level from  $^{247}\text{Cm}$  to  $^{253}\text{No}$ , which is getting steeper towards increasing proton numbers. Therefore, our result may be regarded qualitatively as in line with the prediction, solely the “steeper” decrease sets in at a lower proton number. The assignment of the asymptotic quantum number for the 558 keV level in  $^{251}\text{Fm}$ , was based on the low hindrance factor for the  $\alpha$  transition into this level indicating a “favoured” transition (see table 2). So a change in the assignment of the 558 keV level would require also a change of the ground-state assignment of the  $\alpha$ -decay precursor  $^{255}\text{No}$ , which does not seem to be justified so far due to the similar  $\alpha$ -decay properties of  $^{251}\text{Cf}$  [16, 22],  $^{253}\text{Fm}$  [19, 16], and  $^{255}\text{No}$ . The further increase of the energy for the  $1/2^+[620]$  state to  $^{253}\text{No}$  is less certain, since it is based on hindrance factors of  $^{257}\text{Rf}$   $\alpha$  decays having very weak relative intensities [25]. Here much more sensitive measurements are necessary to draw reliable conclusions.

Finally, spin and parity assignment of the tentative level at 394 keV in  $^{251}\text{Fm}$  are  $3/2^+$ . On the basis of the theoretical calculations an appropriate choice thus would be the  $3/2^+[622]$  Nilsson level. However, this state so far has not been identified in the lighter and more detailed investigated  $N = 151$  isotones  $^{247}\text{Cm}$  and  $^{249}\text{Cf}$  at  $E^* < 1\text{ MeV}$ . Since only a smooth variation of its energy as a function of the proton number is predicted (see figs. 5b,c) a “sudden drop” by several hundred keV within  $\Delta Z = 2$  is not expected. Thus, we omit to give asymptotic quantum numbers for this level in fig. 1.

## 4 Summary and conclusion

Our experiments delivered new or enhanced quality data for the decay of  $^{255}\text{No}$ , which improved the level schemes of  $^{251}\text{Fm}$  at low excitation energies and removed some

inconsistencies reported so far. The  $\alpha$  and  $\gamma$  energies are summarized in table 2. The suggested partial level scheme shown in fig. 1 and indicated in fig. 5a is, however, not completely clear. More effort, including also a detailed decay studies of the heavier  $N = 153$  isotones  $^{257}\text{Rf}$  and  $^{259}\text{Sg}$  are necessary. Maximum production cross-sections for the latter isotopes are more than an order of magnitude lower than for  $^{255}\text{No}$ . Respecting that up to date accelerators are able to deliver beams of  $^{48}\text{Ca}$ ,  $^{50}\text{Ti}$  or  $^{54}\text{Cr}$  with intensities of up to one  $p\mu\text{A}$  improved data can be measured in experimental runs of two to three weeks, which is presently typical for “heavy element” experiments. To obtain high-precision data, however, new devices, delivering dc beams of several  $p\mu\text{A}$  are necessary. A significant increase of the beam intensity is also necessary to overcome a severe handicap of the implantation method: energy summing of  $\alpha$  particles and conversion electrons render the identification of levels and the measurement of their energy quite difficult if they decay predominantly by internal conversion. To reduce this effect a separation of the “source” and the detector is necessary, which, however, must be expected to go along with a loss of efficiency. One possibility is to stop the evaporation residues after in-flight separation in a gas cell and to transport them to an appropriate detection system. This method has been already successfully applied for chemical investigations [31]. A more rigorous method is to couple an in-flight separator with an ion trap, which allows, in addition, for a precise measurement of the mass, as it has been realized at SHIP-TRAP [32]. This device has been already applied successfully for mass measurements in the range  $A \approx (90\text{--}150)$  and it is planned to extend the experimental program to the region of heaviest nuclei in the near future.

We want to express our gratitude to H.G. Burkhard and H.J. Schött for skillful maintenance of the mechanical and electrical components of SHIP. We thank the UNILAC staff as well as K. Tinschert and the “ion source crew” for delivering beams of high and stable intensity and the excellent performance of the accelerator. We are also grateful to J. Steiner, W. Hartmann and A. Hübner for production of the large area targets and preparation of the target wheels. The work was supported by EURONS, contract number RII3-CT-2004-506065.

## References

1. M. Leino, F.P. Heßberger, *Annu. Rev. Nucl. Part. Sci.* **54**, 175 (2004).
2. F.P. Heßberger, S. Hofmann, D. Ackermann, V. Ninov, M. Leino, G. Münzenberg, S. Saro, A. Lavrentev, A.G. Popeko, A.V. Yeremin, Ch. Stodel, *Eur. Phys. J. A* **12**, 57 (2001).
3. F.P. Heßberger, S. Hofmann, D. Ackermann, P. Cagarda, R.-D. Herzberg, I. Kojouharov, P. Kuusiniemi, M. Leino, R. Mann, *Eur. Phys. J. A* **22**, 417 (2004).
4. B. Kindler, D. Ackermann, W. Hartmann, F.P. Heßberger, S. Hofmann, B. Lommel, R. Mann, J. Steiner, to be published in *Nucl. Instrum. Methods Phys. Res. A*.



5. H. Folger, W. Hartmann, F.P. Heßberger, S. Hofmann, J. Klemm, G. Münzenberg, V. Ninov, W. Thalheimer, P. Armbruster, Nucl. Instrum. Methods A **362**, 65 (1995).
6. G. Münzenberg, W. Faust, S. Hofmann, P. Armbruster, K. Güttner, H. Ewald, Nucl. Instrum. Methods **161**, 65 (1979).
7. S. Hofmann, V. Ninov, F.P. Heßberger, P. Armbruster, H. Folger, G. Münzenberg, H.J. Schött, A.G. Popeko, A.V. Yeremin, A.N. Andreyev, S. Saro, R. Janik, M. Leino, Z. Phys. A **350**, 277 (1995).
8. S. Hofmann, W. Faust, G. Münzenberg, W. Reisdorf, P. Armbruster, K. Güttner, H. Ewald, Z. Phys. A **291**, 53 (1979).
9. S. Hofmann, G. Münzenberg, Rev. Mod. Phys. **72**, 733 (2000).
10. F.P. Heßberger, S. Hofmann, D. Ackermann, Eur. Phys. J. A **16**, 365 (2003).
11. F.P. Heßberger, S. Hofmann, G. Münzenberg, K.-H. Schmidt, P. Armbruster, R. Hingmann, Nucl. Instrum. Methods A **274**, 522 (1989).
12. F.P. Heßberger, S. Antalic, B. Streicher, S. Hofmann, D. Ackermann, B. Kindler, I. Kojouharov, P. Kuusiniemi, M. Leino, B. Lommel, R. Mann, K. Nishio, S. Saro, B. Sulignano, Eur. Phys. J. A **26**, 133 (2005).
13. D.N. Poenaru, M. Ivascu, M. Mazila, J. Phys. (Paris), Lett. **41**, 589 (1980).
14. E. Rurarz, Acta Phys. Pol. B **14**, 917 (1983).
15. A.A. Chasman, I. Ahmad, A.M. Friedman, J.R. Erskine, Rev. Mod. Phys. **49**, 833 (1977).
16. R.B. Firestone, V.S. Shirley, C.M. Baglin, S.Y. Frank Chu, J. Zipkin, *Table of Isotopes* (John Wiley & Sons, Inc., New York, Chichester, Brisbane, Toronto, Singapore, 1996).
17. R.S. Hager, E.C. Seltzer, Nucl. Data A **4** (1968).
18. P. Eskola, K. Eskola, M. Nurmi, A. Ghiorso, Phys. Rev. C **2**, 1058 (1970).
19. I. Ahmad, A.M. Friedman, R.F. Barnes, R.K. Sjoblom, J. Milsted, P.R. Fields, Phys. Rev. **164**, 1537 (1967).
20. P.F. Dittner, C.E. Bemis jr., D.C. Hensley, R.J. Silva, C.D. Goodman, Phys. Rev. Lett. **26**, 1037 (1971).
21. C.E. Bemis jr., D.C. Hensley, P.F. Dittner, C.D. Goodman, R.J. Silva, ORNL **4708**, 62 (1971).
22. I. Ahmad, R.R. Chasman, J.P. Greene, F.G. Kondev, E.F. Moore, E. Browne, C.E. Porter, L.K. Felker, Phys. Rev. C **68**, 044306 (2003).
23. A. Ghiorso, M. Nurmi, J. Harris, K. Eskola, P. Eskola, Phys. Rev. Lett. **22**, 1317 (1969).
24. C.E. Bemis jr., R.J. Silva, D.C. Hensley, O.L. Keller jr., J.R. Tarrant, L.D. Hunt, P.F. Dittner, R.L. Hahn, C.D. Goodman, Phys. Rev. Lett. **31**, 647 (1973).
25. F.P. Heßberger, S. Hofmann, V. Ninov, P. Armbruster, H. Folger, G. Münzenberg, H.J. Schött, A.G. Popeko, A.V. Yeremin, A.N. Andreyev, S. Saro, Z. Phys. A **359**, 415 (1997).
26. B. Streicher, PhD Thesis, Comenius University Bratislava (submitted, June 2006).
27. P. Reiter, T.L. Khoo, I. Ahmad, A.V. Afanasjev, A. Heinz, T. Lauritsen, C.J. Lister, D. Seweryniak, P. Bhattacharyya, P.A. Butler, M.P. Carpenter, A.J. Chewter, J.A. Cizewski, C.N. Davids, J.P. Greene, P.T. Greenlees, K. Helariutta, R.-D. Herzberg, R.V.F. Janssens, G.D. Jones, R. Julin, H. Kankaanpää, H. Kettunen, F.G. Kondev, P. Kuusiniemi, M. Leino, S. Siem, A.A. Sonzogni, J. Uusitalo, I. Wiedenhoever, Phys. Rev. Lett. **95**, 032501 (2005).
28. S. Cwiok, S. Hofmann, W. Nazarewicz, Nucl. Phys. A **573**, 356 (1994).
29. A. Parkhomenko, A. Sobiczewski, Acta Phys. Pol. **36**, 3115 (2005).
30. P. Möller, J.R. Nix, W.D. Myers, W.J. Swiatecki, At. Data Nucl. Data Tables **59**, 185 (1995).
31. J.P. Omtvedt, J. Alstad, H. Breivik, J.E. Dyve, K. Eberhardt, C.M. Folden III, T. Ginter, K.E. Gregorich, E.A. Hult, M. Johansson, U.W. Kirbach, D.M. Lee, M. Mendel, A. Nähler, V. Ninov, L.A. Omtvedt, J.B. Patin, G. Skarnermark, L. Stavsetra, R. Sudowe, N. Wiehl, B. Wierczinski, P.A. Wilk, P.M. Zielinski, J.V. Kratz, N. Trautmann, H. Nitsche, D. Hoffman, J. Nucl. Radiochem. Sci. **3**, 121 (2002).
32. S. Rahaman, M. Block, D. Ackermann, D. Beck, A. Chaudhuri, S. Eliseev, H. Geissel, D. Habs, F. Herfurth, F.P. Heßberger, S. Hofmann, G. Marx, M. Mukherjee, J.B. Neumayr, M. Petrick, W.R. Plaß, W. Quint, C. Rauth, D. Rodriguez, C. Scheidenberger, L. Schweickhard, P.G. Thirolf, C. Weber, Int. J. Mass Spectrom. **251**, 146 (2006).